Preparation of High-Modulus and High-Strength Isotactic Polypropylene Fiber by Zone-Annealing Method

TOSHIO KUNUGI, TAIHEI ITO, MINORU HASHIMOTO, and MASASHI OOISHI, *Department of Applied Chemistry, Faculty of Engineering, Yamanashi University, Takeda-4, Kofu-shi, 400 Japan*

Synopsis

The zone-annealing method was utilized to prepare a high-modulus and high-strength fiber from isotactic polypropylene. The dynamic storage modulus at room temperature of the fiber obtained reached 21×10^{10} dyn/cm^2, which corresponded to 51% of the crystal modulus along the molecular chains, 41.2×10^{10} dyn/cm^2. The relationships between mechanical properties and superstructure were investigated based on results of measurements of orientation, crystallinity, tensile properties, and dynamic viscoelasticity. It was found that the excellent mechanical properties were directly attributed to the large number of tie molecules and to the high orientation of the amorphous chains. Further, the characteristics of this method were discussed compared with the results obtained by other investigators.

INTRODUCTION

Research on the preparation of fibers or films with high modulus and high strength have been very actively carried out with considerable interest in the relationships between superstructure and mechanical properties. A variety of techniques, such as superdrawing,[1,2] high pressure extrusion,[3–5] spinning of fibers from liquid crystals[6] or flowing polymer solutions,[7] gel-state spinning,[8] and hot drawing.[9]

The authors have also proposed a new method termed the "zone-annealing method".[10] The method has so far been applied to poly(ethylene terephthalate),[10–15] nylon 6,[10–12,16–20], and polyethylene[11,12,21] and clearly has a remarkable effect on improving the mechanical properties of these polymers.

In this paper, we wish to report on the results of the application of this method to isotactic polypropylene.

EXPERIMENTAL

Material

The original material used in this study was as-spun isotactic polypropylene fiber of about 0.5 mm diameter supplied by Mitsubishi Rayon Co. The fiber has a birefringence of 2.4×10^{-3}, a crystallinity of 57.9%, $\overline{M}_n = 8.17 \times 10^4$, and $\overline{M}_w = 4.75 \times 10^5$.

Journal of Applied Polymer Science, Vol. 28, 179–189 (1983)

CCC 0021-8995/83/010179-11$02.10

Zone Drawing and Zone Annealing

The procedure of the zone-annealing method consists of two stages of zone drawing and zone annealing. The zone drawing was done in order to fully arrange the molecular chains, whereas the zone annealing was subsequently carried out to crystallize the fibers in a bundle state. The apparatus used in the present study was the usual tensile tester partially reconstructed. A band heater 2 mm in width was attached to a movable crosshead. The upper end of the fiber was fixed, and the desired high tension was then applied to the fiber by weighting. The band heater was held at a suitable temperature and then was moved up or down along the fiber axis at a desirable speed.

At first the zone drawing and zone annealing were carried out only once, under conditions which will be described later. However, one-step procedures still seem to be insufficient to extend and arrange the molecular chains. The as-spun isotactic polypropylene fiber has a high crystallinity (57.9%) and contains a large number of lamellae. In order to more effectively unfold the lamellae, therefore, it is necessary to repeat the zone drawing and zone annealing. As will be shown later, the zone drawing was repeated five times and the zone annealing 12 times under suitable conditions. In this study, these multistep zone-drawing and zone-annealing processes are abbreviated as MZD and MZA. In contrast to this, one-step procedures are indicated by 1ZD and 1ZA.

Measurements

The tensile properties were measured at 23–25°C, RH 65%, on a monofilament 20 mm long. Young's modulus, the tensile strength, and the elongation at break were estimated from the stress–strain curves. The dynamic viscoelastic properties, storage modulus E', loss modulus E'', and loss tangent tan δ were measured at 110 Hz. The measurements were carried out in two temperature ranges: from 0°C to 130°C and from 0°C to −130°C. The higher temperature measurements were performed at a heating rate of 2°C/min in a stream of dry air. The lower temperature measurements were done at a cooling rate of 2°C/min in a stream of dry air cooled with liquid nitrogen.

The birefringence was measured with a polarizing microscope equipped with Berek's compensator. The density was measured at 25°C by a flotation method using water–methyl alcohol mixtures. The crystallinity was calculated from the density by the usual method using a crystal density[22] of 0.936 and an amorphous region density[22] of 0.850 g/cm^3.

The orientation factor of crystallites, f_c, was determined by X-ray diffraction. The bundle of fibers was placed on a fiber holder mounted in the usual X-ray diffractometer. The measurements of reflection intensity in the radial direction were made at intervals of 1° or 10° from the equator to the meridian. The intensities obtained were corrected for polarization, absorption, background noise, and incoherent scattering. Further, the amorphous contribution and the overlapping components arising from the adjacent crystal planes were separated from the corrected intensities according to Kawai's procedure.[23] An example is shown in Figure 1. From the azimuthal intensity distributions thus obtained, the orientation factors of normals of the (110) and (040) planes, f_{110} and f_{040}, were evaluated by the usual method.[24] Further, by substituting the values of f_{110} and

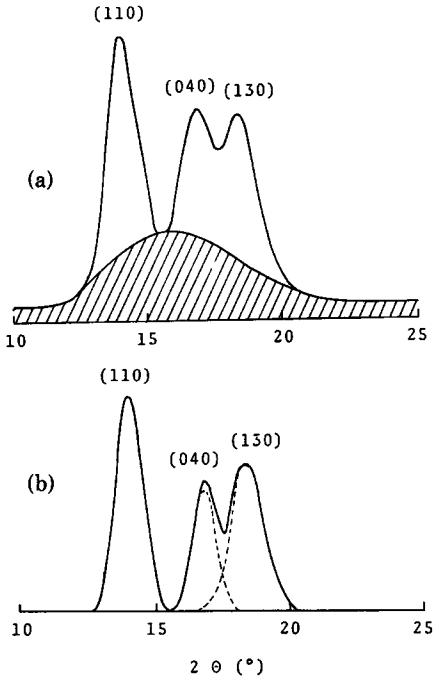

Fig. 1. An example of the separation of crystalline and amorphous X-ray scattering intensities. (a) Separation of amorphous contribution from the total X-ray scattering intensity. The shaded part indicates the amorphous contribution. (b) Separation of the crystalline contribution into those of the (110), (040), and (130) crystal planes.

f_{040} into the following equation, the orientation factor of crystallites f_c was calculated:

$$f_c = \frac{2(f_{110} \cos 2\psi_{040} - f_{040} \cos 2\psi_{110})}{\cos 2\psi_{110} - \cos 2\psi_{040}}$$

where ψ_{110} and ψ_{040} are the angles between the b axis and the normals of the (110) and (040) planes.

The orientation factor of the amorphous chains f_a was calculated from the following equation by substituting the values of crystallinity (X_c), birefringence (Δ_t), and f_c measured separately.

$$f_a = \frac{\Delta t - X_c f_c \Delta_c^0}{(1 - X_c)\Delta_a^0}$$

where Δ_c^0 and Δ_a^0 are the intrinsic birefringences of the crystal[25] and the amorphous phase,[25] 0.0331 and 0:0468, respectively.

RESULTS AND DISCUSSION

Determination of Suitable Conditions

In the zone-annealing method, a variety of variables ranging from molecular weight, its distribution, and processing history of the original fiber, to heating

method and structure of the heater may be considered. The search for fully satisfactory conditions, therefore, seems almost hopelessly complicated. In the present study, we have concentrated on the temperature and moving speed of the heater, the tension applied on the fiber, and the number of repetitions of zone drawing and zone annealing, as done in the previous studies.[10–14,17,20,21]

A large number of preliminary experiments were performed. Table I shows examples of preliminary experiments for zone drawing. The purpose of zone drawing is to obtain a highly oriented fiber. However, if the drawing temperature is too high, crystallization occurs at the same time, whereas if the tension is too high, whitening or severance of the fiber occurs. In Table I, the relationships among the temperature of the heater, the tension applied on the fiber, and the draw ratio of the drawn fiber are shown, which were obtained at a heater moving speed of 40 mm/min.

When the temperature or tension was too low, the fiber could not be drawn, whereas when these were too high, the necking portion was out of the heater. From Table I, it is found that the highest draw ratio is realized at a drawing temperature of 70°C under a tension of about 2 kg/mm^2. Similarly, the most suitable conditions for zone annealing were determined to be a temperature of 130°C and a tension of about 12 kg/mm^2.

Furthermore, the multistep procedure was attempted. The zone drawing was repeated five times gradually increasing the tension from 1.59 to 15.9 kg/mm^2 at 70°C with a heater moving speed of 40 mm/min. The zone annealing was also repeated six times under two tensions of 10.5 and 20.0 kg/mm^2, respectively. By adopting such a multistep procedure, the tension applicable to the fibers increased remarkably, i.e., from 2.08 to 11.9 kg/mm^2 for zone drawing and from 15.9 to 20.0 kg/mm^2 for zone annealing. These conditions are summarized in Table II.

Tensile Properties

Table III shows Young's modulus, tensile strength, and elongation at break of the fibers prepared by the one-step procedure and the multistep procedure. Young's modulus increases rapidly by zone drawing and zone annealing in both procedures. In particular, the values increase threefold over those of the zone-drawn fibers by zone annealing. It is also found that the tensile properties of the fibers prepared by the multistep procedure are definitely superior to those

TABLE I
Effects of Heater-Temperature and Applied Tension at Zone-Drawing on Draw Ratio (Times)[a]

Tension (kg/mm^2)	Heater temperature (°C)						
	40	50	60	70	80	90	100
0.72	xxx	xxx	xxx	xxx	xxx	xxx	3.7
0.96	xxx	xxx	xxx	xxx	3.6	3.9	4.4
1.20	xxx	xxx	xxx	4.0	4.3	4.4	4.9
1.44	xxx	xxx	3.8	4.2	4.7	5.2	- - -
1.68	xxx	3.7	4.4	4.9	5.2	- - -	- - -
1.92	- - -	4.6	5.3	5.8	- - -	- - -	- - -
2.16	- - -	- - -	- - -	- - -	- - -	- - -	- - -

[a] (xxx) Unstretching; (- - -) cold drawing at the outside of heating zone.

TABLE II
Most Suitable Conditions for Zone Drawing and Zone Annealing

Conditions	1ZD[a]	MZD[b] (1)	(2)	(3)	(4)	(5)	1ZA[c]	MZA[d] (1–6)	(7–12)
Temp of heating zone (°C)	70			70			130	130	
Moving speed of heater (mm/min)	40			40			20	20	
Tension applied to fiber (kg/mm^2)	2.08	1.59	7.35	9.80	12.1	15.9	11.9	10.5	20.0
Repetition (times)	1	1	1	1	1	1	1	6	6

[a] 1ZD: 1-step zone drawing.
[b] MZD: multistep zone drawing.
[c] 1ZA: 1-step zone annealing.
[d] MZA: multistep zone annealing.

by the one-step procedure. The maximum value of Young's modulus, 17.2 × 10^{10} dyn/cm^2, is 2.9–3.3 times that of commercially available fibers, 5.2–6.0 × 10^{10} dyn/cm^2.

On the other hand, the maximum value of tensile strength is 75.8 kg/mm^2, which is far higher than that of the commercial fiber, 40–48 kg/mm^2. Because all of the fibers were invariably broken at the portions near the clamps on testing, we expect that the real strength value will be much higher.

Dynamic Viscoelastic Properties

Figures 2 and 3 show the temperature dependence of the dynamic storage modulus E' in the higher and lower temperature ranges, respectively. The E' value is still low in the zone-drawing stage but is rapidly increased by zone annealing over all the temperature ranges.[26] Also the multistep procedure can be said to be definitely superior to the one-step procedure for increasing the modulus. The maximum value at room temperature reaches 21 × 10^{10} dyn/cm^2, which corresponds to 51% of the crystal modulus, 41.2 × 10^{10} dyn/cm^2, which was measured using X-ray reflection of the (003) crystal plane by Sakurada et al.[27] In addition, the fiber which was prepared by the multistep procedure ex-

TABLE III
Tensile Properties of Original Fiber, Zone-Drawn Fibers, and Zone-Annealed Fibers

Sample		Young's modulus (× 10^{-10} dyn/cm^2)	Strength at break (kg/mm^2)	Elongation at break (%)
Original fiber		0.91	—	—
Zone-drawn fiber	1ZD[a]	3.82	38.1	36.3
	MZD[b]	5.57	46.2	29.8
Zone-annealed fiber	1ZD–1ZA[c]	12.60	59.5	8.7
	MZD–MZA[d]	17.20	75.8	8.8

[a] 1ZD: 1-step zone drawing.
[b] MZD: multistep zone drawing.
[c] 1ZD–1ZA: 1-step zone annealing after 1ZD.
[d] MZD–MZA: multistep zone annealing after MZD.

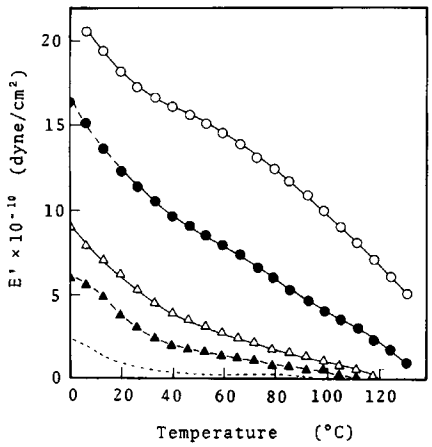

Fig. 2. Temperature dependence of the dynamic storage modulus E' in the higher temperature range for the five kinds of fibers: (- - - -) original fiber; (▲) 1ZD; (△) MZD; (●) 1ZD–1ZA; (○) MZD–MZA.

hibits a high E' value even at high temperatures: for example, 5×10^{10} dyn/cm^2 at 130°C.

In the lower temperature range, we could not observe any isolated dispersion peak. However, in the higher temperature range, two dispersion peaks appeared at about 8°C and in the vicinity of 80°C, as seen in Figure 4. The lower temperature peak corresponds to the α_a dispersion, whereas the higher temperature peak represents the α_c dispersion. The intensities of the peaks increase step by step in the order of the original fiber, the zone-drawn fiber, and the zone-annealed fiber. In particular, the α_c peak grows rapidly and shifts to higher temperatures. Since this behavior means an increase in quantity and an im-

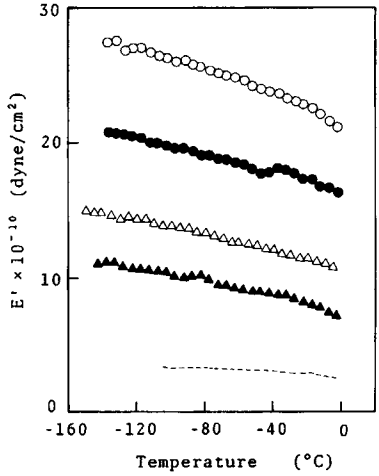

Fig. 3. Temperature dependence of the dynamic storage modulus E' in the lower temperature range for the five kinds of fibers: (- - - -) original fiber; (▲) 1ZD; (△) MZD; (●) 1ZD–1ZA; (○) MZD–MZA.

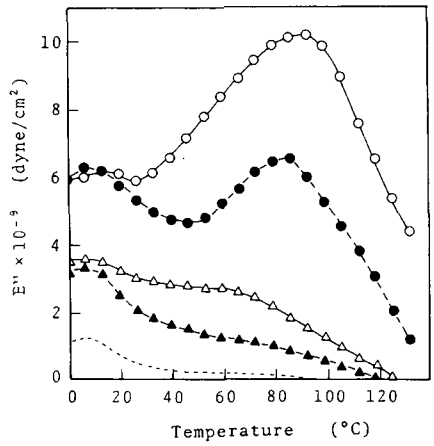

Fig. 4. Temperature dependence of the loss modulus E'' in the higher temperature range for the five kinds of fibers: (- - - -) original fiber; (▲) 1ZD; (△) MZD; (●) 1ZD–1ZA; (○) MZD–MZA.

provement in quality, respectively, it can be considered that the multistep zone-annealed fiber contains numerous high-quality crystallites. This suggestion is also based on the results of DSC measurement. In the same order, the melting peak becomes steeper and shifts to higher temperatures. Comparison of the melting points is shown in Table IV. We think that, in the higher temperature range, the crystallites prevent movement and relaxation of the amorphous chains and contribute directly to maintenance of the high modulus.

Orientation and Crystallinity

To elucidate the relationships between the mechanical properties and the superstructure in each stage, the orientation and crystallinity were examined. Figure 5 shows the X-ray Laue photographs, while Table V lists the birefringence (Δ_t), the orientation factors (f_c and f_a), and the crystallinity (X_c) for the five kinds of fibers.

Compared with the data on mechanical properties in Table IV or Figures 2 and 3, it is found that these superstructural factors are arranged in the same order of increasing magnitude as obtained for the modulus and the tensile strength.

TABLE IV
Melting Point of Original Fiber, Zone-Drawn Fibers, and Zone-Annealed Fibers

Sample		Melting point (°C)
Original fiber		160.0
Zone-drawn fiber	1ZD[a]	161.5
	MZD[b]	161.5
Zone-annealed fiber	1ZD–1ZA[c]	163.0
	MZD–MZA[d]	164.0

[a] 1ZD: 1-step zone drawing.
[b] MZD: multistep zone-drawing.
[c] 1ZD–1ZA: 1-step zone annealing after 1ZD.
[d] MZD–MZA: multistep zone annealing after MZD.

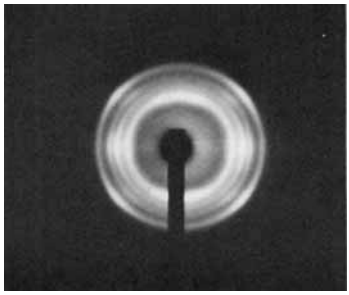

Original fiber

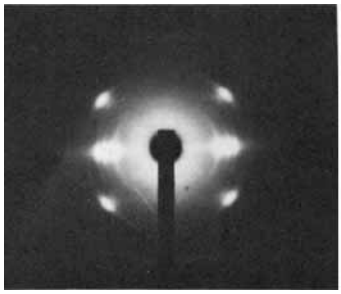

1ZD

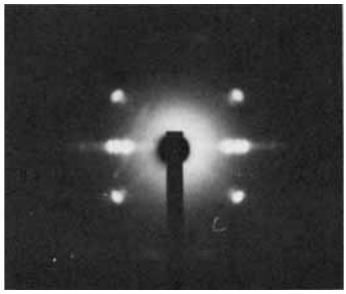

MZD

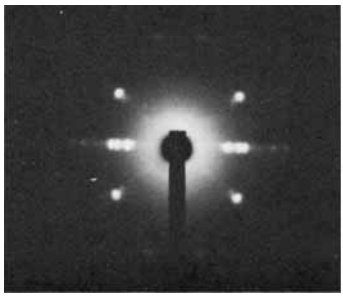

1ZD-1ZA

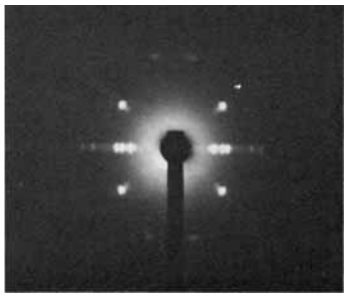

MZD-MZA

Fig. 5. X-ray Laue photographs of the five kinds of fibers.

When examined in further detail, it is found that f_c easily reaches a very high value by zone drawing but increases only slightly by zone annealing. Also, the increment in increase in the X_c is small. In contrast to f_c and X_c, f_a increases steadily with the processing and is proportional to Young's modulus and the E'. This fact suggests that the increase in f_a contributes greatly to the improvement in mechanical properties.

Estimation of Amorphous Modulus and Number and Fraction of Tie Molecules

As noted in the previous papers,[14,15,17,21] if the crystalline region is not completely continuous along the fiber axis, the amorphous region which has a lower

TABLE V
Birefringence (Δ_t), Orientation Factors of Crystallites and Amorphous Chains (f_c and f_a), and Crystallinity (X_c) of Original Fiber, Zone-Drawn Fibers, and Zone-Annealed Fibers

Sample		$\Delta_t \times 10^3$	f_c	f_a	X_c
Original fiber		2.4	—	—	57.9
Zone-drawn fiber	1ZD[a]	30.4	0.970	0.605	54.8
	MZD[b]	31.5	0.985	0.634	59.5
Zone-annealed fiber	1ZD–1ZA[c]	34.0	0.988	0.825	62.2
	MZD–MZA[d]	36.9	0.990	0.957	65.6

[a] 1ZD: 1-step zone drawing.
[b] MZD: multistep zone drawing.
[c] 1ZD–1ZA: 1-step zone annealing after 1ZD.
[d] MZD–MZA: multistep zone annealing after MZD.

modulus has a more pronounced influence on the mechanical properties of the semicrystalline polymer materials. Therefore, we again estimated the amorphous modulus (E_a) and the number and fraction of the tie molecules [$(1 - X_c)E_\parallel/E_{c\parallel}$ and β_E], using the same procedure as that the previous papers.[15,18–21]

The values obtained are shown in Table VI. All of these values vary in proportion to the moduli and tensile strength. This strongly suggests that the increase in tie molecules results in an increase in E_a, and further the increase in E_a leads to a distinct improvement in the mechanical properties. This interpretation is identical to those previously obtained for the other polymers.[15,18–21]

In Table VII, these values are compared for the four kinds of polymers. From the results, the following differences can be seen. First, the isotactic polypropylene fiber has the largest quantity of tie molecules. The amorphous modulus, nevertheless, is significantly smaller than that of polyethylene. This suggests that the herical conformation of the molecular chains promotes unfolding of the lamellae because of the weak intermolecular force but is not simultaneously effective in producing a high modulus, compared with the planar zigzag conformation of polyethylene molecular chains. However, because the crystal modulus is also small, the extent of approach of the attainable modulus to the crystal

TABLE VI
Amorphous Modulus (E_a), Number and Fraction of Tie Molecules [$(1 - X_c)E_\parallel/E_{c\parallel}$ and β_E] of Original Fiber, Zone-Drawn Fibers, and Zone-Annealed Fibers]

Sample		E_a ($\times 10^{-10}$ dyn/cm^2)	$(1 - X_c)E_\parallel/E_{c\parallel}$	β_E
Original fiber		0.38	0.012	0.027
Zone-drawn fiber	1ZD[a]	1.73	0.050	0.111
	MZD[b]	2.50	0.066	0.162
Zone-annealed fiber	1ZD–1ZA[c]	6.36	0.142	0.376
	MZD–MZA[d]	8.82	0.172	0.501

[a] 1ZD: 1-step zone drawing.
[b] MZD: multistep zone drawing.
[c] 1ZD–1ZA: 1-step zone annealing after 1ZD.
[d] MZD–MZA: multistep zone annealing after MZD.

TABLE VII
Comparisons of Amorphous Modulus (E_a) Number and Fraction of Tie Molecules [$(1 - X_c)E_\parallel/E_{c\parallel}$ and β_E] in Four Kinds of Semicrystalline Polymers

Polymer	E_a ($\times 10^{-10}$ dyn/cm^2)	$(1 - X_c)/E_\parallel/E_{c\parallel}$	β_E
Nylon 6	5.6	0.034	0.067
PET	8.7	0.072	0.180
PE	15.9	0.056	0.223
it-PP	8.8	0.172	0.501

modulus, 51%, becomes markedly higher than that of polyethylene, 23%, because of the effect of the tie molecules.

Comparison with Maximum Modulus Values Reported by Other Investigators

In the case of isotactic polypropylene, also, many techniques for preparing high modulus and high strength materials have so far been reported.[28–35] Table VIII shows the proposed techniques and the maximum modulus values obtained at room temperature. Values above 20×10^{10} dyn/cm^2 have been reported by Taylor and Clark[33] and Coates and Ward.[35]

Taylor and Clark[33] prepared an isotactic polypropylene fiber with a high modulus of 22×10^{10} dyn/cm^2 by a two-step drawing process. The method consists of two stages. In the first stage, an unoriented extruded billet is rapidly drawn in a natural draw ratio of about sevenfold in hot sillicon oil. In the second stage, the fiber is drawn at a very low speed of 4%/min and at a carefully controlled temperature of 130°C up to 25-fold.

On the other hand, Coates and Ward[35] examined the die-drawing technique. By using an extended nose, they obtained a product with Young's modulus up to 20.6×10^{10} dyn/cm^2 by die drawing of $R_N = 7$ and 15 mm die at 110°C. The draw ratio was about 20-fold.

By the zone-annealing method, we obtained a room temperature dynamic modulus of 21×10^{10} dyn/cm^2 comparable to these values, despite the simple apparatus, the easy procedure, the relatively high speed, and the fairly low draw ratio of about 12-fold. Further, our method may be repeated and continuously

TABLE VIII
Comparison of Maximum Modulus Values Reported by Various Investigators

Investigator		Method	Maximum modulus ($\times 10^{-10}$ dyn/cm^2)
Noether and Singleton[28]	(1964)	Multistep drawing	14
Sheehan and Cole[29]	(1964)	Hot drawing	10
Williams[30]	(1973)	Hydrostatic extrusion	17
Desper[31]	(1973)	Hot drawing	16
Cansfield, Capaccio, and Ward[32]	(1976)	Super drawing	19
Taylor and Clark[33]	(1978)	Two-step drawing	22
Kamezawa et al.[34]	(1979)	Zone drawing	15
Coates and Ward[35]	(1979)	Die drawing	20.6
Kunugi et al.[a]	(1982)	Zone annealing	21

[a] The present paper and Ref. 26.

operated under a series of tensions and speeds. Recently, we obtained a still higher modulus of 23.1×10^{10} dyn/cm^2 by "zone melting" at a far higher temperature of 180°C and at a lower speed of 2 mm/min. The fiber also exhibited a tensile strength of 116.7 kg/mm^2, a birefringence of 37.1×10^{-3}, and a crystallinity of 71.2%. These details will be reported in the near future.

References

1. N. J. Capiati and R. S. Porter, *J. Polym. Sci., Polym. Phys. Ed.*, **13,** 1177 (1975).
2. G. Capaccio and I. M. Ward, *Polymer*, **15,** 233 (1974).
3. N. E. Weeks and R. S. Porter, *J. Polym. Sci., Polym. Phys. Ed.*, **12,** 635 (1974).
4. P. D. Griswold and J. A. Cuculo, *J. Appl. Polym. Sci.*, **22,** 163 (1978).
5. A. G. Gibson and I. M. Ward, *J. Polym. Sci., Polym. Phys. Ed.*, **16,** 2015 (1978).
6. S. L. Kwolek, U.S. Pat. 3,671,542 (1972).
7. A. Zwijnenburg and A. J. Pennings, *Colloid Polym. Sci.*, **254,** 868 (1976).
8. B. Kalb and A. J. Pennings, *J. Mater. Sci.*, **15,** 2584 (1980).
9. W. Wu and W. B. Black, *Polym. Eng. Sci.*, **19,** 1163 (1979).
10. T. Kunugi, A. Suzuki, I. Akiyama, and M. Hashimoto, *Polym. Prepr., Am. Chem. Soc. Div. Polym. Chem.*, **20,** 778 (1979).
11. T. Kunugi, *Sen-i Gakkaishi*, **36,** 411 (1980).
12. T. Kunugi, *Chem. Ind. (Jpn.)*, **32,** 289 (1981).
13. T. Kunugi, *New Materials and New Processes*, JEC Press, Cleveland, Oh., 1981, Vol. 1, p. 58.
14. T. Kunugi, A. Suzuki, and M. Hashimoto, *J. Appl. Polym. Sci.*, **26,** 213 (1981).
15. T. Kunugi, A. Suzuki, and M. Hashimoto, *J. Appl. Polym. Sci.*, **26,** 1951 (1981).
16. T. Kunugi, *Polymer*, **23,** 176 (1982).
17. T. Kunugi, I. Akiyama, and M. Hashimoto, *Polymer*, **23,** 1193 (1982).
18. T. Kunugi, I. Akiyama, and M. Hashimoto, *Polymer*, **23,** 1199 (1982).
19. T. Kunugi, T. Ikuta, M. Hashimoto, and K. Matsuzaki, *Polymer*, to appear.
20. T. Kunugi, *Sen-i Gakkaishi*, **38,** P-257 (1982).
21. T. Kunugi, I. Aoki, and M. Hashimoto, *Kobunshi Ronbunsyu*, **38,** 301 (1981).
22. J. Brandrup and E. H. Immergut, *Polymer Handbook*, Wiley, New York, 1975, p. V-23.
23. H. Takahara, H. Kawai, and T. Yamada, *Sen-i Gakkaishi*, **23,** 102 (1967); G. Natta, *J. Polym. Sci.*, **34,** 351 (1959).
24. Z. W. Wilchinsky, *J. Appl. Phys.*, **30,** 792 (1959).
25. R. J. Samuels, *J. Polym. Sci., Part A*, **3,** 1741 (1965).
26. T. Kunugi, *J. Polym. Sci., Polym. Lett. Ed.*, **20,** 329 (1982).
27. I. Sakurada, T. Ito, and K. Nakamae, *J. Polym. Sci., C*, **15,** 75 (1966).
28. H. D. Noether and R. W. Singleton, U.S. Pat. 3,161,709 (1964).
29. W. C. Sheehan and T. B. Cole, *J. Appl. Polym. Sci.*, **8,** 2359 (1964).
30. T. Williams, *J. Mater. Sci.*, **8,** 59 (1973).
31. C. R. Desper, *J. Macromol. Sci., Phys. Ed.*, **B7,** 105 (1973).
32. D. L. M. Cansfield, G. Capaccio, and I. M. Ward, *Polym. Eng. Sci.*, **16,** 721 (1976).
33. W. N. Taylor and E. S. Clark, *Polym. Eng. Sci.*, **18,** 518 (1978).
34. M. Kamezawa, K. Yamada, and M. Takayanagi, *J. Appl. Polym. Sci.*, **24,** 1227 (1979).
35. P. D. Coates and I. M. Ward, *Polymer*, **20,** 1553 (1979).

Received June 1, 1982
Accepted July 26, 1982